American Mineralogist, Volume 65, pages 1166–1175, 1980

The solubility behavior of CO_2 in melts on the join $NaAlSi_3O_8$–$CaAl_2Si_2O_8$–CO_2 at high pressures and temperatures: a Raman spectroscopic study

BJØRN O. MYSEN AND DAVID VIRGO

Geophysical Laboratory, Carnegie Institution of Washington
Washington, D.C. 20008

Abstract

The solubility behavior of CO_2 in melts on the join $CaAl_2Si_2O_8$–$NaAlSi_3O_8$–CO_2 has been determined at high pressures and temperatures by Raman spectroscopy and beta-track autoradiography. The carbon dioxide dissolves predominantly as a metal carbonate complex in such melts and is 25 percent more soluble in $CaAl_2Si_2O_8$ than in $NaAlSi_3O_8$ melt at the same pressure and temperature. The Raman spectra of quenched $NaAlSi_3O_8$ + CO_2 melt indicate that some carbon dioxide is also dissolved as molecular CO_2.

The CO_2-free melts consist of two 3-dimensional aluminosilicate network units. In both $CaAl_2Si_2O_8$ and $NaAlSi_3O_8$ melt these two units become enriched in Si relative to Al as carbon dioxide is dissolved. In addition, there is a third structural unit with both Si and Al in tetrahedral coordination and with nonbridging oxygens. A consequence of the formation of a metal carbonate complex is that some of the aluminum in the melt is not in tetrahedral coordination in melts of $CaAl_2Si_2O_8$ + CO_2 and $NaAlSi_3O_8$ + CO_2 composition.

Introduction

Carbon dioxide has attracted the attention of igneous petrologists because of its influence on phase equilibria relevant to partial melting in the upper mantle (*e.g.*, Yoder, 1973; Eggler, 1973, 1975, 1978; Eggler and Rosenhauer, 1978; Huang and Wyllie, 1976; Wendlandt and Mysen, 1978; Mysen and Boettcher, 1975a,b). Some of these authors have shown that the presence of CO_2 in the upper mantle results in partial melts that contain less silica than those formed in the absence of CO_2. It has also been noted (*e.g.*, Eggler, 1973) that the presence of CO_2 during fractional crystallization tends to enhance the stability of minerals that are more polymerized than the liquidus minerals in CO_2-free systems. Subsequent studies of CO_2-solubility mechanisms in relevant melt compositions have shown that in melts that contain a significant number of nonbridging oxygens per tetrahedral cation (NBO/T), CO_2 is dissolved in the form of a carbonate complex (Mysen *et al.*, 1975, 1976; Brey and Green, 1976; Eggler *et al.*, 1979). The carbonate ion was interpreted to be closely associated with metal cations such as Ca^{2+} and Mg^{2+} in (Ca,Mg) meta- and orthosilicate melts (Eggler and Mysen, 1976; Holloway *et al.*, 1976; Mysen and Virgo, 1980). As a result of the formation of such carbonate complexes, the number of nonbridging oxygens per tetrahedral cation in the melt has decreased. In other words, CO_2 solution in such melts results in polymerization of the melt.

Melts on the joins $NaAlO_2$–SiO_2 and $CaAl_2O_4$–SiO_2 contain the petrologically important plagioclase components. It is necessary, therefore, to understand the solubility mechanisms of CO_2 in such melts before the role of CO_2 in magmas can be completely understood. Determinations of carbon dioxide solubility in melts on the join $NaAlO_2$–SiO_2–CO_2 have shown that several weight percent CO_2 may dissolve in these melts at high temperatures and pressures and that at least some of this CO_2 exists as CO_3^{2-} (Mysen, 1976). Inasmuch as CO_2-free melts on this join have NBO/T = 0 (Mysen *et al.*, 1980a), the influence of dissolved CO_2 on the melt structure must differ from that for melts with NBO/T > 0. The melt compositions on the joins $NaAlO_2$–SiO_2 and $CaAl_2O_4$–SiO_2 are also important because possible contrasting roles of Na^+ and Ca^{2+} on CO_2-solubility mechanisms may be observed. We decided, therefore, to integrate studies of CO_2 solubility with Raman spectroscopy to determine the structural role of CO_2 in melts with no nonbridging oxygens.

0003–004X/80/1112–1166$02.00

Experimental techniques

The starting materials were spectroscopically pure SiO_2, Al_2O_3, and $CaCO_3$ to make melts of $CaAl_2Si_2O_8$ (An) composition with CO_2 in solution. The carbonate was the source of CO_2. The composition An + CO_2 contains 13.66 wt. percent CO_2. Experiments with this composition were therefore conducted in the presence of excess CO_2 when the CO_2 solubility in the melt did not exceed 13.66 wt. percent CO_2. The $NaAlSi_3O_8$ + CO_2 composition (Ab + CO_2) was made from spectroscopically pure SiO_2 and Al_2O_3 and reagent-grade Na_2CO_3. The Na_2CO_3 was the source of CO_2 (8.60 wt. percent CO_2 in the starting material). Both An + CO_2 and Ab + CO_2 melting experiments were conducted in the presence of a nearly pure CO_2 vapor phase.

All experiments were carried out in a solid-media, high-pressure apparatus (Boyd and England, 1960) with a 0.5″ diameter furnace contained within a Pyrex-glass sleeve. The furnace parts were thoroughly dried prior to the experiments to minimize the availability of H_2O, which dissociates to H_2 and O_2 during the experiments. The H_2 may enter the sample through the walls of the sealed Pt sample containers. Eggler *et al.* (1974) found that with the technique used here, the vapor contains at least 99 mole percent CO_2 (less than 1 mole percent CO and H_2O) after an experiment.

A −4 percent friction correction was applied to the experiments (calibrated against the quartz–coesite transition). The piston-out technique was used. The uncertainty of the pressure is ±1 kbar (Eggler, 1977).

The temperatures were measured with a Pt–Pt90Rh10 thermocouple with no correction for pressure on the electromotive force. The latter simplification results in an uncertainty in the temperature reading of 6°–10°C depending on the temperature at $P > 10$ kbar (Mao *et al.*, 1971).

The carbon contents (reported as CO_2) of the melts were measured with beta-track counting (Mysen and Seitz, 1975). Carbon-14 was used as beta-active isotope, and K-5 nuclear emulsions were used as detectors (supplied by Ilford Inc., England). The analytical uncertainty is 2–3 percent relative to the amount present (Mysen and Seitz, 1975; Mysen, 1976; Kadik and Eggler, 1975; Eggler *et al.*, 1979).

All aspects of the experiments pertaining to equilibrium CO_2 contents were performed according to the methods described by Mysen and Seitz (1975), Mysen *et al.* (1976), and Mysen and Virgo (1980). We consider, therefore, that the CO_2 contents were measured at equilibrium. The possible presence of trapped stable CO_2 vapor in quenched melts of Ab composition was discussed by Mysen (1976) and Mysen *et al.* (1976). They concluded that trapped stable CO_2 vapor most likely would not affect the analytical results. Possible problems with exsolution of vapor during quenching are discussed later.

All details of the Raman spectroscopic procedures have been described by Mysen *et al.* (1980a). The Raman spectra have been deconvoluted into individual bands according to the procedures discussed by Mysen *et al.* (1980a).

Melt vs. quenched melt

Both carbon analysis and spectroscopic measurements were carried out on quenched samples. It is necessary, therefore, to assess whether the quenching process has affected the carbon concentrations in the melts and the structural features that can be discerned with Raman spectroscopy.

Carbon analysis of quenched melts of a variety of bulk compositions has been compared with carbon contents determined with chemographic techniques (Mysen *et al.*, 1976; Kadik and Eggler, 1975; Eggler *et al.*, 1979). The compositional range, temperatures, and pressures of our experiments were covered by those studies. The results indicate that the carbon dioxide contents of the quenched melts equal those of the melts themselves.

In order to relate the structural information from quenched melts to structural features of silicate melts, it must be demonstrated that the features under consideration are not significantly affected by the quenching. Riebling (1968) and Taylor *et al.* (1980) found that anionic structural units (silicate polymers) in melts with a 3-dimensional network structure such as melt of $NaAlSi_3O_8$ composition remain the same as the melt is quenched. Direct experimental proof of structural similarity between melts and their quenched analogues on the join Na_2O–SiO_2 was provided by Sweet and White (1969) and Sharma *et al.* (1978). In those studies, infrared and Raman spectra of melts of $Na_2Si_3O_7$, $Na_2Si_2O_5$, and Na_2SiO_3 composition were compared with those of their quenched equivalents. It was concluded that the structures of these melts were not affected by the quenching process.

On the basis of the information given above, we conclude that both structural features discernible with Raman spectroscopy and carbon concentrations determined by beta-track mapping are quenchable. The results on quenched melts given in this report

are believed to be applicable, therefore, to liquid silicates.

Results

Carbon dioxide solubility in melts of Ab composition is shown as a function of temperature and pressure in Table 1. The results agree with those of Mysen (1976) within the temperature and pressure ranges covered in both studies. The carbon dioxide solubility increases from about 1 wt. percent at 10 kbar to about 3 wt. percent at 30 kbar and 1650°C. The solubility increases isobarically with increasing temperature, as also found by others for other compositions (*e.g.*, Mysen *et al.*, 1975, 1976; Eggler, 1973; Holloway *et al.*, 1976). The CO_2 solubility at given temperature and pressure is less than in any melt containing nonbridging oxygen studied to date.

Carbon dioxide contents of An melt are shown as a function of pressure in Table 1. We note by comparing data in Table 1 that the CO_2 solubility in An melt is about 25 percent greater than in Ab melt at the same pressure and temperature. Furthermore, the data in Table 1 indicate that the CO_2 solubility in An melt may decrease with increasing temperature at temperatures above 1750°C. The temperature dependence of CO_2 solubility could not be determined at lower temperatures because of the high liquidus temperatures in the system $CaAl_2Si_2O_8$–CO_2. Mysen and Virgo (1980) suggested that the fugacity of CO_2 may decrease with increasing temperature above about 1700°C at $P(CO_2)$ greater than 10 kbar, a conclusion that agrees with MRK data for CO_2 by Holloway (1977). In that case, the CO_2 solubility in the melt will also decrease with increasing temperature, as observed by Mysen and Virgo (1980) and Holloway *et al.* (1976) for meta- and orthosilicate melts, and now for An melt. We conclude, therefore, that the negative temperature dependence of CO_2 solubility in An melt at $P(CO_2) = 25$ kbar and $T > 1750$°C is a result of the lowering of $f(CO_2)$ and is not due to solubility mechanisms of CO_2 in the melt at these high temperatures.

The high-frequency envelopes of the Raman spectra of quenched An + CO_2 melt as a function of CO_2 content are shown in Figure 1. Detailed data from the complete spectral region are shown in Table 2. The high-frequency envelope of CO_2-free quenched An melt at 20 kbar consists of two (Si,Al)-coupled, asymmetric stretch bands (993 and 930 cm^{-1}, respectively) indicative of two 3-dimensional structural units in the melt (Mysen *et al.*, 1980b). The band at the highest frequency (993 cm^{-1}) reflects

Table 1. CO_2 contents and other run data

Comp.	P, kbar	T, °C	Run Duration, min.	Wt % CO_2	Mole % CO_2 (O=8)
Ab	10	1650	5	0.68±0.02	3.92
Ab	20	1650	5	1.87±0.04	10.19
Ab	20	1700	5	2.05±0.05	11.09
Ab	20	1750	5	2.22±0.05	11.91
Ab	30	1450	15	2.06±0.04	11.13
Ab	30	1550	15	2.31±0.04	12.34
Ab	30	1650	5	2.87±0.09	14.96
Ab	30	1700	5	3.20±0.05	16.44
Ab	30	1750	5	3.53±0.13	17.89
An	10	1750	5	1.34±0.03	7.74
An	15	1750	5	1.98±0.05	11.32
An	20	1750	5	2.68±0.08	14.82
An	25	1750	5	3.61±0.09	19.13
An	25	1790	5	2.94±0.09	16.06

stretch vibrations in the most aluminous structural unit. Addition of CO_2 to this melt results in the development of a shoulder near 1070 cm^{-1} (Fig. 1). This shoulder becomes more pronounced with increasing CO_2 content. In the deconvoluted spectra [see Mysen *et al.* (1980a) for discussion of deconvolution procedures] it can be seen (Fig. 1) that this shoulder is due to a broad band near 1075 cm^{-1}. A sharp band near 1075 cm^{-1} was also found in CO_2-saturated melts of $CaMgSi_2O_6$ (Di) and $NaCaAlSi_2O_7$ (Sm) composition by Mysen and Virgo (1980). They concluded, as did White (1974) and Verweij *et al.* (1977) for other compositions, that this is a C–O stretch band characteristic of the CO_3^{2-} anion. There is no band near 1300 cm^{-1} to indicate the presence of molecular CO_2 (Rosasco and Simmons, 1974) in An + CO_2. The broadness of the C–O stretch band in these melts compared with the form of the band in less polymerized silicate melts may indicate considerably more disorder (variable bond lengths and bond angles) of the CO_3^{2-} complex in quenched An + CO_2 melt than in melts of Di + CO_2 and Sm + CO_2.

The frequency of the two (Si,Al)–O^0 bands remains essentially constant with increasing CO_2 content of the quenched An melt (Fig. 1). This result indicates that the Al/(Al + Si) of the individual 3-dimensional units does not change appreciably. The intensity ratio, $I(1100)/I(1000)$, decreases (Fig. 2). This decrease indicates that the proportion of the most aluminous 3-dimensional structural unit decreases relative to that of the more silica-rich unit as carbonate complexes are formed in the melt.

From a spectroscopic point of view, the high-frequency envelope of quenched An + CO_2 can be satisfied with the three bands discussed above. In this case, the bulk Al/(Al + Si) of the melt must have decreased [the intensity ratio, $I(1100)/I(1000)$, de-

creases with increasing CO_2 content]. This decrease of Al/(Al + Si) can be accomplished in two ways. The carbonate complex may be stabilized as an aluminum carbonate complex. If this is the case, an amount of Ca^{2+} equivalent to the aluminum in the carbonate complex is no longer needed to charge-balance Al^{3+} in the 3-dimensional network. This Ca^{2+} is now a network modifier, thus producing non-

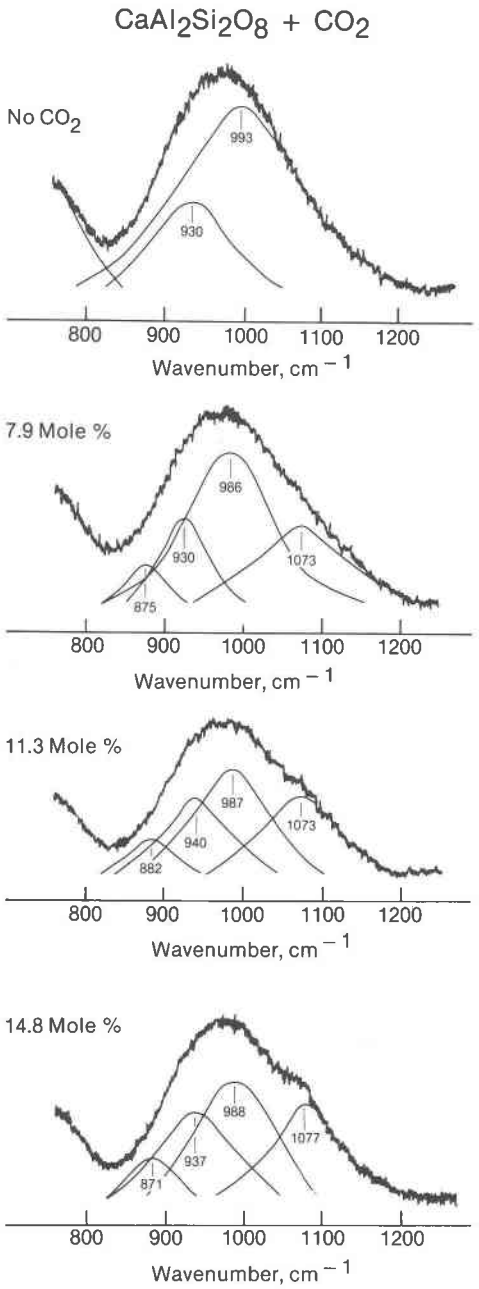

Fig. 1. Raman spectra of quenched melts in the system $CaAl_2Si_2O_8$–CO_2 as a function of CO_2 content (calculated on the basis of 8 oxygens).

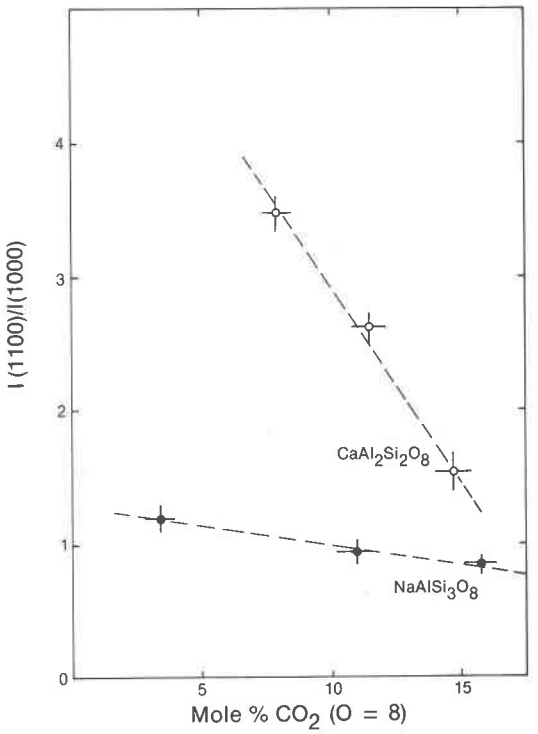

Fig. 2. Shifts of intensity ratio $I(1100)/I(1000)$ as a function of mole percent CO_2 (O = 8) in solution for melts of Ab + CO_2 and An + CO_2 composition.

bridging oxygens in the melt. Such a mechanism has been proposed for the solution of P_2O_5 in An melt, for example (Mysen *et al.*, 1980b).

An alternative explanation for the decreased bulk Al/(Al + Si) is that the carbonate is a calcium carbonate complex much like that found in quenched Di and Sm melts with CO_2 (Mysen and Virgo, 1980). If this solution mechanism is correct, an amount of Al^{3+} equivalent to that needed to form the $(CaCO_3)^0$ complex in the melt is no longer charge-balanced in tetrahedral coordination and will leave the network (Mysen *et al.*, 1980a). As this Al^{3+} leaves the network, the Al/(Al + Si) of the remaining 3-dimensional units will have decreased and new nonbridging oxygens will be formed in the melt.

In summary, the existence of CO_3^{2-} and the decrease of Al/(Al + Si) in the three-dimensional network units in quenched An + CO_2 melt require that nonbridging oxygens have been formed. Structural units with NBO result in stretch vibrations that have Raman bands at lower frequencies than Raman bands from structural units with no nonbridging oxygen (Furukawa and White, 1980). As a result of these considerations, a fourth band was fitted in the high-frequency envelope of the Raman spectrum of

quenched An + CO_2 melt. This band occurs between 870 and 880 cm^{-1} (Fig. 1).

The 870 cm^{-1} band may result from a sheet or a chain unit in the melt. If the band reflects the presence of a sheet unit, the band has shifted from 1050–1100 cm^{-1}, which is the frequency of Al-free, $^{-}O–Si–O^{0}$ stretching[1] (Furukawa and White, 1980; Verweij, 1979) to 870 cm^{-1} as a function of Al content of the unit. If the 870 cm^{-1} band reflects the presence of a chain unit in the melt, the shift would have been from about 950 cm^{-1} ($^{-}O–Si–O^{-}$ asymmetric stretch; Verweij, 1979; Furukawa and White, 1980) as a consequence of the Al content of the structural unit. A choice between these alternatives cannot be made from the spectroscopic data.

In summary, the Raman spectroscopic data in Figure 1 are interpreted to indicate that solution of carbon dioxide in melt of An composition at high pressure and temperature results in the formation of carbonate complexes. In addition, the melt consists of two discrete 3-dimensional network units that have become depleted in Al relative to the CO_2-free melt. Furthermore, a third aluminum silicate unit with nonbridging oxygens has been formed.

The high-frequency envelope of Raman spectra of quenched melts in the system $NaAlSi_3O_8$–CO_2 is shown in Figure 3, and detailed data are given in Table 2. The Raman spectrum of CO_2-free, quenched Ab melt at 20 kbar is discussed by Mysen *et al.* (1980a). The high-frequency envelope of that spectrum is shown here for comparison (Fig. 3). There are two (Si,Al)–O^0 stretch bands at 1083 and 984 cm^{-1}, where the 1083 cm^{-1} band is due to the 3-dimensional structural unit with the largest Al/(Al + Si) (Virgo *et al.*, 1979). The structures of An and Ab melt without CO_2 differ only in the Al/(Al + Si) of the two 3-dimensional structural units (Virgo *et al.*, 1979).

At 10 kbar and 1650°C, 3.9 mole percent CO_2 dissolves in Ab melt (Table 1). The Raman spectra of such melts have two distinct bands at 1272 and 1377 cm^{-1} with an intensity ratio, $I(1272)/I(1377)$, near 0.6. The frequencies and the intensity ratio are characteristic of molecular CO_2 (Herzberg, 1945). There is no clear spectroscopic evidence for more than two bands in the high-frequency envelope. The two

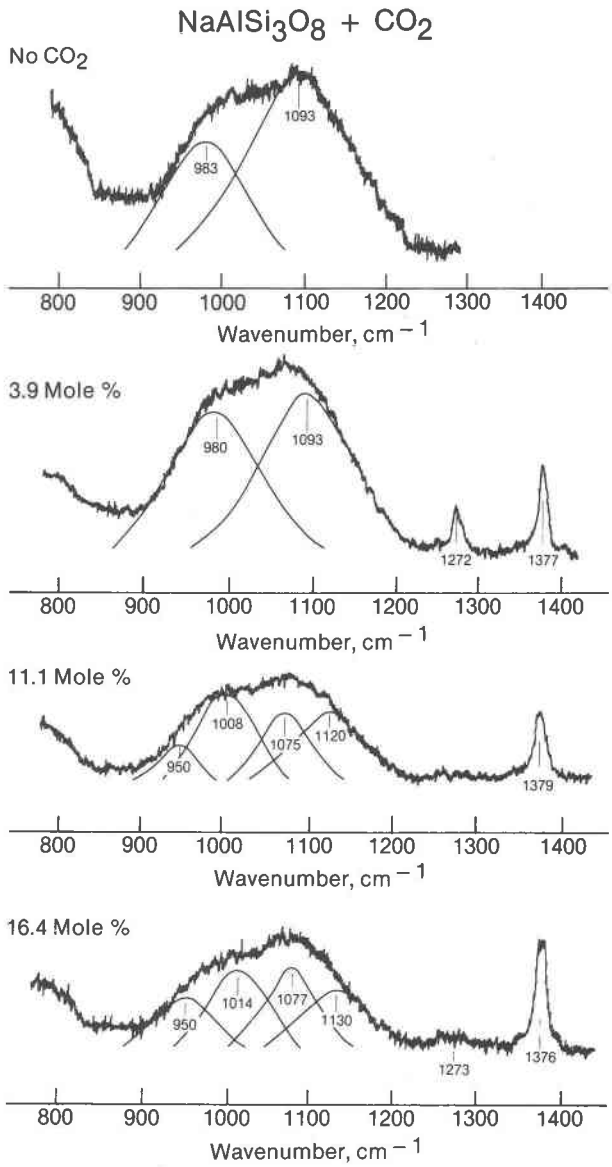

Fig. 3. Raman spectra of quenched melts of Ab + CO_2 composition as a function of CO_2 content (calculated as mole percent on the basis of 8 oxygens).

(Al,Si)–O^0 stretch bands occur at the same frequency as in the absence of CO_2. The Al/(Al + Si) of the two 3-dimensional structural units is therefore not affected. The intensity ratio $I(1100)/I(1000)$ of quenched Ab + 3.9 mole percent CO_2 is greater than in the absence of CO_2 (Table 2), and therefore the bulk Al/(Al + Si) of the 3-dimensional aluminum silicate units may have been reduced (Mysen *et al.*, 1980a). In view of the above discussion of the structure of quenched An + CO_2, the latter observation indicates that some CO_3^{2-} may be present in quenched Ab melt with 3.9 mole percent CO_2. In the

[1] The notations $^{-}O–Si–O^{-}$, $^{0}O–Si–O^{-}$, and $Si–O^{0}$ refer to vibrations across an oxygen bond involving two, one, and no nonbridging oxygens, respectively, in the tetrahedron. Such vibrations are characteristic of chain, sheet, and 3-dimensional structural units. The notation (Si,Al) *etc.* implies the presence of Al in tetrahedral coordination.

Table 2. Raman spectroscopic data

Composition	P, kbar	T, °C	Wavenumber, cm^{-1}*									$I(1100)/I(1000)$†
An	20	1760	513s	580(sh)	765(sh)	...	930m	993s	...	...	...	3.72
An + CO_2	10	1750	500s	580(sh)	786(sh)	875w	930m	986s	1073m	...	...	3.23
An + CO_2	15	1750	500s	570(sh)	786(sh)	882w	940m	987s	1073s	...	...	2.62
An + CO_2	20	1750	500s	570(sh)	780(sh)	871w	937m	988s	1077s	...	...	1.53
Ab	20	1450	468s	573(sh)	794(sh)	...	983m	1093s	...	...	...	2.06
Ab + CO_2	10	1650	470s	567w	786(sh)	950w	980s	1093s	...	1273m	1377s	1.18
Ab + CO_2	20	1700	468s	567w	780(sh)	...	1008s	1120s	1075s	...	1379s	0.94
Ab + CO_2	30	1700	473s	568(sh)	783(sh)	950m	1014s	1130s	1077s	...	1376s	0.84

Abbreviations: (sh), shoulder; w, weak; m, medium; s, strong.

†*The $I(1100)/I(1000)$ reflects the $I(990)/I(930)$ in melts of An composition and $I(1100)/I(1000)$ in melts of Ab composition.*

absence of a band near 1070 cm^{-1} in the raw Raman spectrum, no such band was fitted.

The addition of 11.1 mole percent CO_2 (calculated on the basis of 8 oxygens) to Ab melt results in several spectroscopic changes. Only one band (at 1379 cm^{-1}) characteristic of molecular CO_2 is observed (Fig. 3). The elimination of the 1272 cm^{-1} band indicates that the symmetry of the CO_2 molecule has changed as the pressure is increased from 10 kbar and the CO_2 content has been increased from 3.9 to 11.1 mole percent.

The high-frequency envelope of quenched Ab + 11.1 mole percent CO_2 indicates the presence of at least three bands. These bands are near 1000, 1070, and 1120 cm^{-1}, respectively (Fig. 3). Bands were fitted near these frequencies. The 1008 and 1120 cm^{-1} bands are the (Si,Al)–O^0 stretch bands indicative of two 3-dimensional structural units (Virgo *et al.*, 1979; Mysen *et al.*, 1980a). Their higher frequencies compared with the spectrum of CO_2-free, quenched Ab melt indicate that the Al/(Al + Si) of both structural units has been lowered. According to the calibration curve of Virgo *et al.* (1979), there is about a 20 percent reduction. The intensity ratio $I(1100)/I(1000)$ of quenched Ab + 11.1 mole percent CO_2 has also decreased relative to its value for quenched Ab + 3.9 mole percent CO_2 and CO_2-free, quenched Ab melt (Fig. 2; see also Table 2). This decrease further indicates a bulk decrease of Al/(Al + Si) of the 3-dimensional portion of the melt.

The 1075 cm^{-1} band is the C–O stretch band characteristic of CO_3^{2-} complexes in quenched Ab + 11.1 mole percent CO_2. In the light of the above considerations, the discussion by Mysen *et al.* (1980a), and the discussion of the spectra of quenched An + CO_2 melt, quenched Ab + 11.1 mole percent CO_2 must contain nonbridging oxygen. The (Si,Al) stretch band reflecting the structural unit with nonbridging oxygen occurs at 950 cm^{-1} (Fig. 3). If this structural unit is of the chain type, its frequency (950 cm^{-1}) coincides with that of ^-O–Si–O^- asymmetric vibrations in Al-free systems (Brawer and White, 1975; Furukawa and White, 1980). Inasmuch as Ab melt contains a large proportion of aluminum, it is likely that this structural unit also contains Al^{3+}. In that case, the NBO/T of this unit must be less than 2. Mysen *et al.* (1980a) concluded that silicate melts relevant to rock-forming processes contain only monomers, dimers, chains, sheets, and 3-dimensional units. In view of the frequency of the 950 cm^{-1} band, it is likely, therefore, that the structural unit with nonbridging oxygen in CO_2-bearing, quenched Ab melt is an aluminous sheet unit.

The Raman spectrum of quenched Ab melt with 16.7 mole percent CO_2 closely resembles that of quenched Ab + 11.1 mole percent CO_2 melt (Fig. 3; see also Table 2). The intensity of the 1075 and 950 cm^{-1} bands has increased somewhat, but their frequencies have remained constant. Thus the proportion of carbonate anion and the structural unit with NBO have both increased with increasing CO_2 content of the melt. Finally, the $I(1100)/I(1000)$ is reduced further as the CO_2 content of the quenched Ab melt has increased from 11.1 to 16.7 mole percent.

In summary, the Raman spectra of quenched Ab + CO_2 melts indicate that the CO_2 is present as molecular CO_2 and as CO_3^{2-} where the proportion of CO_3^{2-} in the melt increases with increasing bulk CO_2 content. There are two 3-dimensional network units whose Al/(Al + Si) decreases as a function of CO_2 content of the melt and a structural unit with NBO/T greater than 0. The proportion of the latter unit also increases with increasing CO_2 content of the melt. With the exception of the possible presence of

dissolved molecular CO_2 in quenched Ab melt, the structures of quenched, CO_2-saturated melts of both $CaAl_2Si_2O_8$ and $NaAlSi_3O_8$ composition are similar.

Solution mechanisms

Before the interaction of CO_2 with the aluminosilicate melt structures is discussed, it is necessary to assess whether the spectroscopic evidence for molecular CO_2 in quenched Ab + CO_2 melt reflects molecular CO_2 in solution or CO_2-rich gas bubbles that are trapped in the quenched melts. Note that Mysen (1976) observed the presence of molecular CO_2 in quenched Ab + CO_2 melt on the basis of infrared measurements. He concluded, from SEM studies of the quenched melts with up to ×20,000 magnification (resolution: 0.005 μm), that the CO_2 is not present as bubbles. That evidence, however, does not rule out the presence of even smaller CO_2 bubbles.

The change of symmetry of the CO_2 molecule with increasing CO_2 concentration indicates that the CO_2 observed in the Raman spectra is related to the melt either as a quench feature (exsolved CO_2 from the melt during quenching) or as dissolved molecular CO_2. If the CO_2 were simply trapped stable vapor from the gas phase present during the experiments, it is unlikely that the gas molecules would be affected by the amount of CO_2 present.

The beta-track maps for carbon-14 indicate that carbon is homogeneously distributed in the quenched melt on an optical scale. Consequently, if the molecular CO_2 results from trapped submicroscopic bubbles, these bubbles must be homogeneously distributed in the sample. In other examples of exsolution of vapor from a melt during quenching, the residual volatile in the quenched melt tends to be heterogeneously distributed. This heterogeneity results from intermittent temperature, pressure, and activity gradients in the melt during the quenching. The consequence of this reasoning is that the molecular CO_2 in quenched Ab + CO_2 melt is, in fact, dissolved in the melt.

It is perhaps more important to determine the role of the carbonate complexes in the quenched melts in the system $CaAl_2Si_2O_8$–$NaAlSi_3O_8$–CO_2. These could be either aluminum or metal carbonate complexes. Silicon carbonate complexes are ruled out on the basis of the increased Si/(Si + Al) of the aluminosilicate portion of the melt and the absence of any Raman bands that could be assigned to Si–O–C stretching. The Si/(Si + Al) of the aluminosilicate portion of the melts would increase whether the carbonate is an aluminum or a metal carbonate, as discussed above. Furthermore, both types of complexes would result in the formation of nonbridging oxygens in the melt. Solubility studies and Raman spectroscopic work on carbon dioxide in (Ca,Mg) ortho- and metasilicate melts at high pressures and temperatures (Holloway *et al.*, 1976; Mysen and Virgo, 1980) indicate that the carbonate complex in those melts is closely associated with the metal cation (Ca^{2+}). We conclude, therefore, that metal carbonate complexes of the type $(CaCO_3)^0$ or $(MgCO_3)^0$ do occur in silicate melts. We also note that in all determinations of the crystal structure of carbonate-bearing silicates the carbonate complex is bonded to the metal cation and not to the silicate framework (Smith, 1953; Smith *et al.*, 1960; Papike and Stephenson, 1966; Canillo *et al.*, 1973; Lin and Burley, 1973; Pluth and Smith, 1973). Finally, we expect that Al–O–C bonds from aluminum carbonate complexes would result in Raman bands in the frequency region between 600 and 700 cm^{-1} (Greenwood, 1975). No such band has been found. We conclude, therefore, that the carbonate complexes in quenched An + CO_2 and Ab + CO_2 melts occur as $(CaCO_3)^0$ and $(Na_2CO_3)^0$ complexes, respectively.

Inasmuch as there is less Al in the 3-dimensional network units of the CO_2-bearing aluminosilicate melts and some of the Na^+ and Ca^{2+} needed for charge balance of Al^{3+} in tetrahedral coordination now are associated with CO_3^{2-}, we conclude that some Al^{3+} may no longer be in tetrahedral coordination in the melts. The amount of such Al^{3+} is equivalent to the amount of carbonate formed in the melt. In An melt, the proportion of such Al^{3+} can be calculated from the CO_2 solubility in the melt because all the CO_2 is dissolved as CO_3^{2-}. The results of such calculations for melts of $CaAl_2Si_2O_8$ composition are shown in Figure 4. A similar calculation may be made for $NaAlSi_3O_8$ (Fig. 4). In the latter case, only maximum values for $Al^*/\Sigma Al$ (Al^* represents Al^{3+} that is no longer in tetrahedral coordination) can be obtained because some of the dissolved carbon exists as molecular CO_2.

The solubility mechanisms for carbonate formation in melt of $NaAlSi_3O_8$ composition may be expressed with the following equation:

$$10NaAlSi_3O_8\ (\text{melt}) + 2CO_2\ (\text{vapor}) = 6NaAlSiO_5^{2-}(\text{sheet}) + (Na_2CO_3)^0\ (\text{melt}) + 4Al^*\ (\text{melt}) + 24SiO_2\ (3D) \quad (1)$$

The entity called SiO_2 ($3D$) represents the increase of

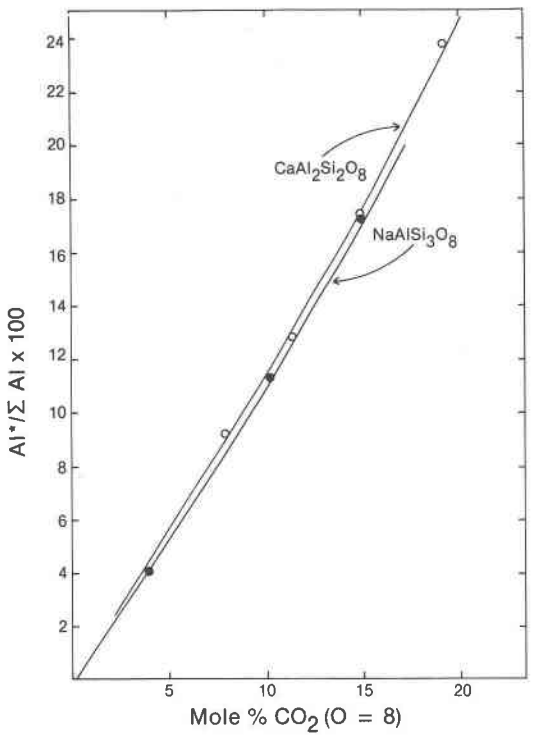

Fig. 4. Proportion (percent) of Al^{3+} not in tetrahedral coordination as a function of CO_2 content (O = 8) of the melt.

Si/(Si + Al) in the 3-dimensional structures as a result of dissolved CO_2. The entity Al* represents the portion of Al^{3+} that is no longer in tetrahedral coordination as a result of dissolved CO_2. This aluminum is now a network-modifier. The entity $(Na_2CO_3)^0$ represents the carbonate complex that has been formed in the melt. In this expression, we assume that Al/Si of the sheet unit in the melt equals 1. If Al/Si < 1, a larger proportion of Al^{3+} is no longer in tetrahedral coordination and some Na^+ will become a network modifier. The Si/(Si + Al) will increase by a smaller amount as a function of increasing CO_2 content. If Al/Si > 1 in the sheet unit in the melt, a smaller proportion of Al^{3+} is no longer in tetrahedral coordination and Si/(Si + Al) will increase at a greater rate with increasing CO_2 content than when Al/Si = 1.

The analogous expression for CO_2 solution in melt of $CaAl_2Si_2O_8$ composition is

$$10CaAl_2Si_2O_8\ (\text{melt}) + 4CO_2 = 6CaAl_2Si_2O_{10}^{4-}\ (\text{sheet}) + 4(CaCO_3)^0\ (\text{melt}) + 8Al^*\ (\text{melt}) + 8SiO_2\ (3D) \quad (2)$$

The solubility mechanism summarized in equations 1 and 2 shows that solution of CO_2 in aluminosilicate melts with 3-dimensional network results in the formation of nonbridging oxygens. Mysen and Virgo (1980) noted that solution of CO_2 in melt of $NaCaAlSi_2O_7$ composition (NBO/T = 0.67) also results in the formation of new nonbridging oxygens through a solution mechanism similar to that shown by equations 1 and 2. This solution mechanism differs from that of melts without amphoteric oxides (*e.g.*, Al_2O_3) for which Mysen and Virgo (1980) found that the following equation can be used to express the solution mechanism:

$$5Si_2O_6^{4-}\ (\text{chain}) + 2CO_2\ (\text{vapor}) = 2SiO_4^{4-}\ (\text{monomer}) + 4Si_2O_5^{2-}\ (\text{sheet}) + 2CO_3^{2-}\ (\text{melt}) \quad (3)$$

Because the ratio of proportions $Si_2O_5^{2-}/SiO_4^{2-}$ in equation 3 is greater than 1, solution of CO_2 in such melts results in a bulk decrease of NBO/T, as first suggested by Eggler (1973) on the basis of phase-equilibrium measurements and solubility studies.

It should be emphasized that in both cases mentioned above the carbonate complex is associated with metal cations. If the metal cation is removed from a charge-balanced complex of Al^{3+} in a silicate polymer, this polymer will be broken up and the melt becomes less polymerized. If the metal cation is a modifying cation in the CO_2-free melt, the melt becomes more polymerized as CO_2 is dissolved.

Applications

Trace-element partition coefficients for transition metals and rare earth elements are very sensitive to NBO/T of the melt. Mysen *et al.* (1980c) have shown, for example, that at 1500°C and 1 atm, K_{Ni}^{Di-liq} decreases in a linear fashion by about 50 percent as NBO/T of the melt increases by about 0.2 unit. Solution of 15–20 mole percent CO_2 (about 2.5 wt. percent) in a melt rich in plagioclase component also results in a decrease of NBO/T of about 0.2 unit. Consequently, nickel partition coefficients between a diopsidic clinopyroxene and a melt that is rich in plagioclase component (*e.g.*, andesite) will decrease by about 50 percent if 2–3 wt. percent CO_2 is dissolved in the melt. Similar calculations can be made for other trace elements (*e.g.*, REE) and other crystal–liquid pairs.

Relatively little is known about phase equilibria of highly polymerized systems in the presence of CO_2. Inasmuch as NBO/T of the melts increases with increasing CO_2 content, it is expected that the liquidus minerals would be less polymerized (less silica-rich) in the presence of CO_2 than in its absence. Pyroxene–plagioclase liquidus boundaries shift toward the silica-deficient portions of systems, for example, as a consequence of this solution mechanism.

Acknowledgments

Critical reviews by D. H. Eggler and H. S. Yoder, Jr. are appreciated. Research was supported partially by NSF grant EAR7911313 and partially by the Carnegie Institution of Washington.

References

Boyd, F. R. and J. L. England (1960) Apparatus for phase-equilibrium measurements at pressures up to 50 kilobars and temperatures up to 1750°C. *J. Geophys. Res., 65,* 741–748.

Brawer, S. A. and W. B. White (1975) Raman spectroscopic investigation of the structure of silicate glasses. I. The binary silicate glasses. *J. Chem. Phys., 63,* 2421–2432.

Brey, G. P. and D. H. Green (1976) Solubility of CO_2 in olivine melilitite at high pressure and the role of CO_2 in the earth's upper mantle. *Contrib. Mineral. Petrol., 55,* 217–230.

Canillo, E., A. Dal Negro and G. Rossi (1973) The crystal structure of latiumite, a new type of sheet silicate. *Am. Mineral., 58,* 466–470.

Eggler, D. H. (1973) The role of CO_2 in melting processes in the mantle. *Carnegie Inst. Wash. Year Book, 72,* 457–467.

——— (1975) Peridotite–carbonatite relations in the system CaO–MgO–SiO_2–CO_2. *Carnegie Inst. Wash. Year Book, 74,* 468–474.

——— (1977) Calibration of a Pyrex solid-media assembly. *Carnegie Inst. Wash. Year Book, 76,* 656–658.

——— (1978) The effect of CO_2 upon melting in the system Na_2O–CaO–Al_2O_3–MgO–SiO_2–CO_2 to 35 kb, with an analysis of melting in a peridotite–H_2O–CO_2 system. *Am. J. Sci., 278,* 305–343.

——— and B. O. Mysen (1976) The role of CO_2 in the genesis of olivine melilitite: discussion. *Contrib. Mineral. Petrol., 55,* 231–236.

——— and M. Rosenhauer (1978) Carbon dioxide in silicate melts. II. Solubilities of CO_2 and H_2O in $CaMgSi_2O_6$ (diopside) liquids and vapors at pressures to 40 kb. *Am. J. Sci., 278,* 64–94.

———, B. O. Mysen and T. C. Hoering (1974) Gas species in sealed capsules in solid-media, high-pressure apparatus. *Carnegie Inst. Wash. Year Book, 73,* 228–232.

———, ———, ——— and J. R. Holloway (1979) The solubility of carbon monoxide in silicate melts at high pressures and its effect on silicate phase relations. *Earth Planet. Sci. Lett., 43,* 321–330.

Furukawa, T. and W. B. White (1980) Raman spectroscopic investigation of the structure of silicate glasses. III. Alkali–silico–germanates. *J. Chem. Phys.,* in press.

Greenwood, N. N. (1975) *Spectroscopic Properties of Inorganic and Organometallic Compounds.* The Chemical Society, London.

Herzberg, G. (1945) *Infrared and Raman Spectra of Polyatomic Molecules.* Van Nostrand Reinhold, New York.

Holloway, J. R. (1977) Fugacity and activity of molecular species in supercritical fluids. In D.G. Fraser, Ed., *Thermodynamics in Geology,* p. 161–187. Reidel, Boston.

———, B. O. Mysen and D. H. Eggler (1976) The solubility of CO_2 in liquids on the join CaO–MgO–SiO_2–CO_2. *Carnegie Inst. Wash. Year Book, 75,* 626–632.

Huang, W.-L. and P. J. Wyllie (1976) Melting relationships in the systems CaO–CO_2 and MgO–CO_2 to 33 kilobars. *Geochim. Cosmochim. Acta, 40,* 129–132.

Kadik, A. A. and D. H. Eggler (1975) Melt–vapor relations on the join $NaAlSi_3O_8$–H_2O–CO_2. *Carnegie Inst. Wash. Year Book, 74,* 479–484.

Lin, S. B. and B. J. Burley (1973) The crystal structure of meionite. *Acta Crystallogr., B29,* 2024–2026.

Mao, H. K., P. M. Bell and J. L. England (1971) Tensional errors and drift of thermocouple electromotive force in the single-stage, piston–cylinder apparatus. *Carnegie Inst. Wash. Year Book, 70,* 281–287.

Mysen, B. O. (1976) The role of volatiles in silicate melts: solubility of carbon dioxide and water in feldspar, pyroxene and feldspathoid melts to 30 kb and 1625°C. *Am. J. Sci., 276,* 969–996.

——— and A. L. Boettcher (1975a) Melting of a hydrous mantle. I. Phase relations of a natural peridotite at high pressures and high temperatures with controlled activities of water, carbon dioxide and hydrogen. *J. Petrol., 16,* 520–548.

——— and ——— (1975b) Melting of a hydrous mantle. II. Geochemistry of crystals and liquids formed by anatexis of mantle peridotite at high pressures and high temperatures as a function of controlled activities of water, hydrogen and carbon dioxide. *J. Petrol., 16,* 549–590.

——— and M. G. Seitz (1975) Trace element partitioning determined by beta-track mapping—an experimental study using carbon and samarium as examples. *J. Geophys. Res., 80,* 2627–2635.

——— and D. Virgo (1980) Solubility mechanisms of carbon dioxide in silicate melts: a Raman spectroscopic study. *Am. Mineral., 65,* 885–899.

———, R. J. Arculus and D. H. Eggler (1975) Solubility of carbon dioxide in natural nephelinite, tholeiite and andesite melts to 30 kbar pressure. *Contrib. Mineral. Petrol., 53,* 227–239.

———, F. J. Ryerson and D. Virgo (1980b) The structural role of phosphorus in silicate melts. *Am. Mineral.,* in press.

———, D. Virgo and C. M. Scarfe (1980a) Relations between the anionic structure and viscosity of silicate melts: a Raman spectroscopic study. *Am. Mineral., 65,* 690–710.

———, ——— and F. Seifert (1980c) Influence of melt structure on element partitioning between olivine and melt and between diopside and melt at 1 atm. *Carnegie Inst. Wash. Year Book, 78,* 542–547.

———, D. H. Eggler, M. G. Seitz and J. R. Holloway (1976) Carbon dioxide in silicate melts and crystals. I. Solubility measurements. *Am. J. Sci., 276,* 455–479.

Papike, J. J. and N. C. Stephenson (1966) The crystal structure of mizzonite, a calcium and carbonate-rich scapolite. *Am. Mineral., 51,* 1017–1027.

Pluth, J. J. and J. V. Smith (1973) The crystal structure of scawtite, $Ca_7(Si_2O_{18})CO_3 \cdot 2H_2O$. *Acta Crystallogr., B29,* 73–80.

Riebling, E. F. (1968) Structural similarities between glass and its melt. *J. Am. Ceram. Soc., 51,* 143–149.

Rosasco, G. J. and J. H. Simmons (1974) Investigation of gas content of inclusions in glass by Raman scattering spectroscopy. *Ceram. Bull., 53,* 626–631.

Sharma, S. K., D. Virgo and B. O. Mysen (1978) Structure of glasses and melts of $Na_2O \cdot xSiO_2$ (x = 1, 2, 3) composition from Raman spectroscopy. *Carnegie Inst. Wash. Year Book, 77,* 649–652.

Smith, J. V. (1953) The crystal structure of tilleyite. *Acta Crystallogr., 6,* 9–18.

———, I. L. Karle, H. Hauptmann and J. Karle (1960) The crystal structure of spurrite, $Ca_5(SiO_4)_2CO_3$. II. Description of structure. *Acta Crystallogr., 13,* 454–458.

Sweet, J. R. and W. B. White (1969) Study of sodium silicate glasses and liquids by infrared spectroscopy. *Phys. Chem. Glasses, 10,* 246–251.

Taylor, M., G. E. Brown and P. M. Fenn (1980) Structure of silicate mineral glasses. III. $NaAlSi_3O_8$ supercooled liquid at 805°C and the effects of thermal history. *Geochim. Cosmochim. Acta, 44,* 109–117.

Verweij, H. (1979) Raman study of the structure of alkali germanosilicate glasses. II. Lithium, sodium and potassium digermanosilicate glasses. *J. Non-Cryst. Solids, 33,* 55–69.

———, H. Van den Boom and R. A. Breemer (1977) Raman scattering of carbonate ions dissolved in potassium silicate glasses. *J. Am. Ceram. Soc., 60,* 529–534.

Virgo, D., B. O. Mysen and I. Kushiro (1980) Anionic constitution of silicate melts quenched at 1 atm from Raman spectroscopy: implications for structure of igneous melts. *Science, 208,* 1371–1373.

———, F. Seifert and B. O. Mysen (1979) Three-dimensional network structures of glasses in the systems $CaAl_2O_4$–SiO_2, $NaAlO_2$–SiO_2, $NaFeO_2$–SiO_2 and $NaGaO_2$–SiO_2 at 1 atm. *Carnegie Inst. Wash. Year Book, 78,* 506–511.

Wendlandt, R. F. and B. O. Mysen (1978) Melting phase relations of natural peridotite + CO_2 as a function of degree of partial melting at 15 and 30 kbar. *Carnegie Inst. Wash. Year Book, 77,* 756–761.

White, W. B. (1974) The carbonate minerals. In V. C. Farmer, Ed., *The Infrared Spectra of Minerals,* p. 227–284. Mineralogical Society, London.

Yoder, H. S., Jr. (1973) Akermanite–CO_2: relationship of melilite-bearing rocks to kimberlite. *Carnegie Inst. Wash. Year Book, 72,* 449–457.

Manuscript received, December 13, 1979;
accepted for publication, May 29, 1980.